Experimental Evaluation of the Solar Flux Distribution on the Flat Receiver of a Model Heliostat System

P. M. Gadhe *‡, S. N. Sapali **, G. N. Kulkarni ***

*Mechanical Engineering, Research Scholar, College of Engineering Pune, Maharashtra-411005, India

***Mechanical Engineering, Professor, College of Engineering Pune, Maharashtra-411005, India

*** Mechanical Engineering, Professor, Government College of Engineering Chandrapur, Maharashtra-442403, India

(prakash.gadhe@mitpune.edu.in, sns.mech@coep.ac.in, govindkulkarni66@gmail.com)

‡Corresponding Author; First Author, Flat no. 402, Sinhagad Darshan Society, Sr. no. 14/4b, wadgaon khurda, Pune, Maharashtra-411041, India,

Tel: +91 9881075970, prakash.gadhe@mitpune.edu.in

Received: 29.01.2018 Accepted:10.04.2018

Abstract- For the efficient utilization of solar energy, its concentration is required. Central Receiver systems have higher concentration ratio as compared to other concentrated solar power techniques. The solar flux density distribution and the temperature on the receiver plate are important parameters in assessing the net thermal energy, in predicting the performance of solar concentrator and in the design of the solar receiver. Here the flux distribution on the flat receiver of the ganged type model heliostat system consisting of nine heliostats has been evaluated by using the thermocouple method which is the indirect method of flux measurement. The variation of the solar flux density distribution on the receiver plate has been estimated for the different numbers of heliostat by using the energy balance equation. For this model heliostat system, the peak flux and average flux values are estimated to be 3950.57 (± 3%) W/m^2 and 1798.77 (± 3%) W/m^2 respectively. This analysis will be useful for sizing of the receiver of solar concentrator. For the average flux value on the receiver plate, the receiver size for the nine heliostats system will be 0.3m x 0.3m with the intercept factor of 64%. The average optical concentration ratio was 5.6 with the optical efficiency of the system 0.50 ± 3 % during the test period.

Keywords - Ganged heliostat, thermocouple method, peak flux, average flux, contours.

1. Introduction

Among all concentrated solar power (CSP) techniques, Central Tower System or Central receiver system (CRS) has higher concentration ratio (CR) as compared to others. In this central tower system, solar radiation is concentrated on a tower mounted receiver by the use of heliostats. These heliostats reflect the radiations at the top of the tower which causes point focus at the center of the receiver. The solar flux incident on receiver heats a heat transfer medium or fluid in the receiver. It can be used to produce the steam which is ultimately used to generate electric power or directly used in the process industries as per the requirement. In this system temperature in the range of 250^{0}C to 1000^{0}C can be obtained at receiver.

The flux density distribution at the focal plane of the receiver is the important term. For the measurement of solar flux on the receiver of the solar concentrating systems two techniques are in use namely indirect and direct. In indirect measurement, camera target method is used that offers a high level of spatial resolution. The concentrated solar radiation falling on the receiver gets reflected from the target is then captured with the use of the camera, generally with a charge-coupled device (CCD) sensor. The image analysis software is used to estimate the flux density distribution on the receiver. Another indirect method in use is the calorimeter method wherein the solar flux is determined by the measurement of heat transfer to a cooling fluid that passes through it. This method is mostly applicable to small-scale heliostat field. In the direct measurement method, a flux sensor or the

radiometer is placed on the receiver that directly gives a measurement signal proportional to the irradiative flux [1, 2].

D. L. King et al. [3] experimentally evaluated the heliostat performance of the Central Receiver Test Facility (CRTF) by using a water-cooled bar with circular foil heat flux gages to measure the flux density. Strachan et al. [4] tested large area heliostats for flux density distribution by using Beam Characterization System (BCS) with CCD camera, Flux Gauge and image analysis software. Ulmer et al. [5] also used the CCD camera and image analysis software without a flux gauge for measuring the flux density distribution from a dish concentrator.

Zhe Dong et al. [6] designed solar flux measurement system with an indirect method which comprises of Lambertian moving bar, a CCD-camera and flux gauges to map the flux density of concentrated solar radiation in the focal plane of solar furnace. O.A. Jaramillo et al. [7] also employed an indirect method for solar flux measurement with the use of cold water calorimetry technique and quantified the solar energy absorbed by the receiver and the heat losses to the surroundings.

Clifford K et al. [8] determined the flux density distribution by using only CCD camera without requiring the additional sensors, calorimeter or flux gauge. To calibrate the pixel values of CCD image the recorded sun image is used which requires rigorous calculations.

A. Ibrahim et al. [9] estimated the solar irradiance on inclined surface facing due south and the method presented, can be used to estimate hourly, global, diffuse solar radiation for horizontal surfaces and total solar radiation on inclined and vertical surfaces at different orientations with greater accuracy for any location. For evaluating the global solar radiation data, prediction of solar radiation and effects on sun positions different, method are given in [10], [11], and [20].

In combination with the water cooled Lambertian target, a thermal infrared imager is used by Xin-LinXia et al. [12] for flux calculation. A flat plate calorimeter is used by Kretzschmar et al. [13] to measure the flux distribution for small-scale heliostat field which requires calculation of heat losses very accurately. Sebastian James Bode et al. [14] used CMOS camera for flux measurement, which is low-cost system as compared to CCD camera and gives good results. Emmanuel Guillot et al. [15] has been carried out the comparison of three heat flux gauges and a water calorimeter for concentrated solar irradiance measurement.

Marc Roger et al. [16] summarizes different techniques to measure solar flux density distribution on large-scale receivers with their advantages and disadvantages. Hyunjin Lee et al. [17] evaluated the optical performance of a solar furnace measuring the concentrating solar flux with the flux mapping method. T. Kodama et. al. [18] measured the concentrated solar flux at the focus point by moving an array of thirteen Gardon gauges.

Miriam Ebert et al. [19] determined the efficiency of SOLUGAS receiver with a major focus on the determination of solar input power. A thermogage radiometers were used for solar flux measurement along with the CCD camera which was positioned in the heliostat field in the optical axis of the receiver. Alain Ferriere et al. [21] designed a flux mapping system which utilizes a flux gauge mounted on the moving bar associated with a CCD camera. This flux mapping system was employed and tested at the top of the Themis solar tower in France.

Anita A. Nene et al. [22] investigated numerically and experimentally Scheffler concentrator receivers for steam generation rate under different operating conditions for process heating application. Dhanesh Jain et al. [23] provided the optimal tilt angle of solar arrays for different locations around the world on the basis of monthly, seasonally, bi-annually and yearly. This review would be beneficial for the further research in solar energy in term of, to identify the optimal tilt angle and collection of radiation for different location in the globe. Mohamed H. Ahmed et al. [24] compared the thermal and optical performance of linear Fresnel and parabolic trough concentrator.

The above methods of flux measurements give accurate flux density distribution but these methods are specialized and require costly instruments. Sharma et al. [25] proposed an indirect and simple flux measurement method called as a thermocouple method which uses the number of thermocouples on the back side of the receiver plate. The temperatures on the flat plate receiver in the focal region of the paraboloidal type of dish receiver are measured to know the radiation flux and its spatial distribution. Kinjavdekar et al. [26] also used this thermocouple method to estimate the flux density distribution on the flat plate receiver of Scheffler dish concentrator.

In the present paper, the flux distribution on the flat receiver of a model heliostat field consisting of nine heliostats was experimentally determined by implementing the thermocouple method proposed by Sharma and Kinjavdekar [25, 26]. Flux distribution is determined by measuring the temperature profile on the flat receiver at the desired focal region of concentrators. The estimation of temperature and flux distribution on the receiver plate is carried out more rigorously by measuring the temperature at an array of large number of points on the receiver plate.

2. Heliostat System

In any general heliostat system, the reflective surface i.e. heliostat is supported on a pedestal which allows its movement about elevation and azimuth axis. For each heliostat, two motors are required to provide power and this power requirement is again vary with the load on heliostat. The heliostat system of which the optical performance is evaluated in this paper is a ganged-type heliostat system [27]. In the ganged type of heliostat system, the numbers of heliostats are mounted on a single actuating rod and are linked mechanically to a rotational shaft. For this type of the system to track the heliostat in a row merely a single DC motor to control the altitudinal (tracking Sun's elevational) movement and another DC motor to control the azimuthal (tracking Sun's azimuthal) movement are required. This is helpful in reducing the cost of motors required in conventional heliostat system. The details of this ganged

heliostat system are available in the patent by Patwardhan et al. [27].

A prototype of this ganged type of heliostat system based on patent [27], was fabricated and the optical performance of this prototype was tested. This prototype consists of a single row of the heliostats system and is composed of 9 heliostats of size 0.60 m x 0.60 m each in a north field configuration. There are three modules of the rotatable shaft of length 4.6 m each and are linearly coupled by interconnecting tubes and flanges. On each rotatable module, three heliostats are mounted and a safe distance between them is kept 0.85 m so that the heliostats should not touch each other during tracking.

3. Methodology

The model of the heliostat system is fabricated and mounted on the terrace of a building as shown in Fig. 1. The position of the center of each heliostat from the ground is kept 1m. The focal length selected for this heliostat system is 7 m. This heliostat structure is composed of an elevation drive which uses a DC motor of torque 28 kg-cm and an azimuthal drive which uses a DC motor of torque 600 kg-cm. These DC motor drives the rotatable shaft to rotate about its axis, such that an array of heliostats mounted on each rotatable shaft rotates tracking an apparent azimuthal motion of the sun in the sky. A stepper motor ball screw linear actuator is connected with the actuating rod on the western aspect of the rotatable shaft & the clockwise rotation of the stepper motor achieves forward (eastward) movement of the actuating rod which in turn causes backward (westward) rotation of mounted heliostats and vice versa.

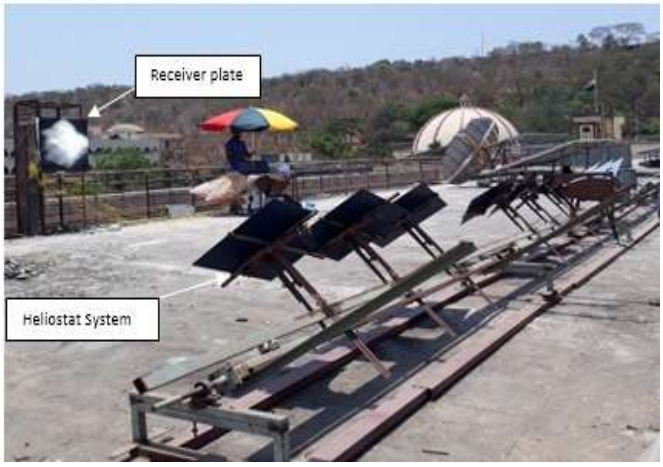

Fig. 1. Heliostat System and the receiver

A mild steel plate (with measured absorptivity α =0.89 and emissivity ε = 0.74) of size 0.9 m x 0.9m and thickness 3mm is used as the receiver plate. The front side of the receiver plate on which the heliostats were focused is coated with a black paint and on the back side of the plate forty-nine blind holes are drilled in a grid of 7x7 with the distance between two consecutive holes is 0.11m. In this blind holes 'K' type thermocouples (expanded uncertainty ± 0.08 ^{0}C) are pasted by high temperature cement which holds the thermocouples in it. Each thermocouple indicates the average temperature of grid area of 0.11m X 0.11m. To suppress the convection and the radiation losses from back side of the receiver a ceramic wool insulation sheet of thickness 25mm (conductivity k = 0.12 W/mK) is applied. The schematic of the thermocouple locations on the receiver plate and the actual plate is shown in Fig. 2 (a) and (b).

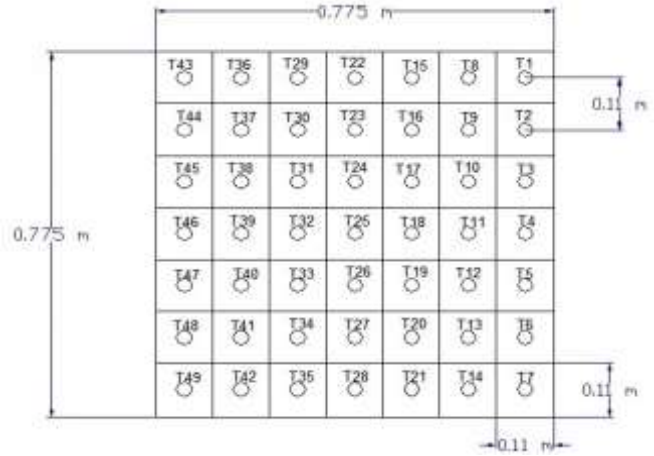

(a)

(b)

Fig. 2. (a) Schematic diagram of the receiver plate with the thermocouple position (b) actual flat receiver plate

Based on the temperature values measured on different locations on the flat plate by thermocouples and using energy balance equation derived for the flat plate, the flux density distribution on the flat surface was estimated [18,19].

The energy balance equation for the small strip of area 0.11m x 0.11 m on the flat plate can be expressed as in Eq. 1-

$$Absorbed\ Energy = Energy\ Loss\ By \begin{Bmatrix} Conduction\ + \\ Convection + \\ Radiation \end{Bmatrix} \quad (1)$$

The final energy balance equation will be given by Eq. 2 as follows [19]-

$$\emptyset_c\,(x) = \frac{[h(T_x - T_{amb}) + \sigma\epsilon(T_x - T_{sky}) + \left(\frac{K_i}{L}\right)(T_x - T_{amb})}{\alpha} \quad (2)$$

From Eq. 1 the solar flux distribution at receiver plane of the heliostat system can be evaluated as a function of temperature measured at that radius.

The beam radiation incident on the aperture mirror surface changes with time of the day so the concentrated flux also varies. This effect of varying beam radiation is normalized by the local concentration ratio $'C(r_i)'$ at a radius $'(r_i)'$ which is defined in Eq. 3.

$$C(r_i) = \frac{\emptyset_c(r_i)}{I_b} \tag{3}$$

The available optical radiation at the annular strip of the focus plate $'d\emptyset_c'$ can be estimated by Eq. 4.

$$d\emptyset_c = \emptyset_c(r_i) 2\pi d(r_i) \tag{4}$$

The optical radiation incident on the plane may also be calculated numerically using Eq. 5 by integrating Eq. 4.

$$d\emptyset_c = \sum_{i=0}^{n} \emptyset_c(r_i)\, A_i \tag{5}$$

Where $'d\emptyset_c'$ the optical radiation at the receiver mouth on the focus plate and $'A_i'$ is the area of the $'i^{th}'$ strip.

The optical efficiency $'\eta_o'$ of the system is defined as in Eq. 6.

$$\eta_o = \frac{\phi_c}{I_b\, A} \tag{6}$$

Where $'I_b'$ is the normal beam radiation and $'A'$ is the aperture area of the concentrator.

3.1. Steps while conducting an experiment

Experimental study was carried out following varying conditions in [28] [29] [30] .The heliostat mirrors were focused on the receiver plate which was placed at the focal point of the heliostat system. By using a data acquisition system the thermocouple readings at various grid locations of the receiver plate were recorded. This data acquisition system records the data of the 45 thermocouples at a time interval of 10sec which is stored in the laptop (in excel sheet format). The solar radiation (global and diffused) were recorded by using radiation pyranometers. Three cup anemometer is used for measuring wind speed, and the air temperature sensor for measuring ambient temperature. All these measuring instruments were mounted near the heliostat system. The data of solar radiation, wind speed, and ambient temperature were recorded in the memory card by using data logger. Before starting the system, all the heliostats were required to be focused manually then the control panel was to be started which tracks the heliostats system automatically during the whole testing period. The experiments were conducted one an half hour before the solar noon and one and half hour after solar noon.

4. Results and Discussion

Based on the temperature values measured at the thermocouple locations on the flat receiver plate, the flux density distribution on the receiver plate is estimated by using the energy balance Eq. (2). Initially, the variation of the flux falling on the receiver plate was estimated by varying the number of heliostats focused. On the first day, the flux measurement testing was carried out by focusing a single heliostat near solar noon. Then the numbers of heliostats were gradually increased in numbers such as three, five, six and nine on each day and the flux measurement near solar noon was carried out. For each case, the flux density distribution was analyzed and the peak flux and the average flux were estimated.

The experimentally estimated flux (W/m^2) contours of density distribution for one, three, five, seven and nine heliostats are shown in Fig. 3.

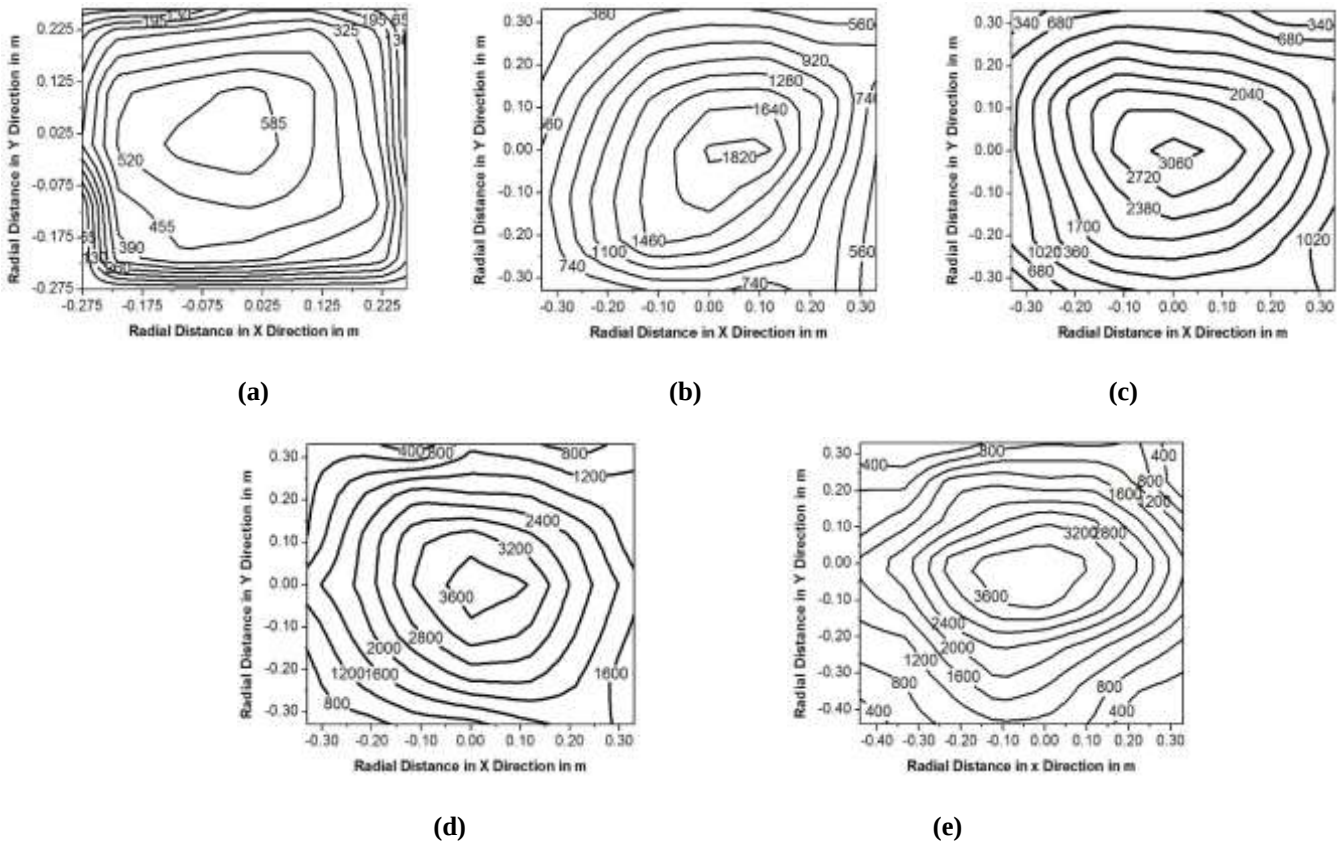

Fig. 3. Flux (W/m^2) contours on the receiver, focusing **(a)** One Heliostats (**b)** Three heliostats **(c)** Five Heliostats **(d)** Seven Heliostats **(e)** Nine Heliostats

It was observed for each case that the peak flux density were value obtained near the center of the receiver plate and flux density gradually decreases from the center to the edges of the receiver. The flux density distribution for each case was following the normal distribution.

To predict the flux values of the increased number of the heliostats in the first row, the peak and the average flux values were normalized by dividing the flux values with the Direct Normal Irradiance (DNI) value at that time and thus the correlation was obtained. Table 1 shows the peak and average flux value for the different number of heliostats.

Table 1. Peak and Average Flux

Total Heliostats numbers focused	Peak flux (W/m^2) (Uncertainty ± 3%)	Average flux (W/m^2) (Uncertainty ± 3%)	DNI (W/m^2)	Normalized peak flux	Normalized average flux
1	637.12	380.26	809	0.79	0.47
3	1885.81	942.38	771	2.45	1.22
5	3201.98	1492.78	803	3.99	1.86
7	3851.13	1852.10	795	4.84	2.33
9	3950.57	1798.77	710	5.56	2.53

The Normalized peak flux and the average flux were plotted against the number of heliostats which is shown in Fig. 4. The correlations obtained from these curves can be used to estimate the peak and the average flux by putting the number of heliostats in the first row of the heliostats. Thus by increasing the number of heliostats above nine in the first row, we can predict the peak and the average flux by using the correlations 7 and 8.

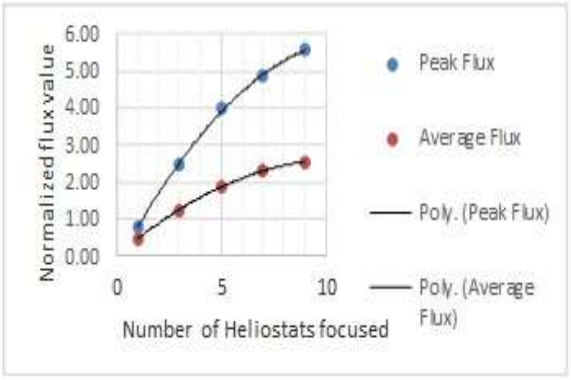

Fig. 4: Variation of flux value

$$Peak\ Flux = -0.0457\,n^2 + 1.055\,n - 0.2397 \quad (7)$$

$$Average\ Flux = -0.0222\,n^2 + 0.4835\,n \quad (8)$$

Where $'n'$ is number of heliostats

By using the above Eqs. (7) and (8), the peak flux value and the average flux value for the increased number of heliostats in the first row is calculated which is shown in the Table 2. The average DNI value for above calculation is taken as 750 W/m^2.

Table 2. Predicted peak and average flux value

Number of Heliostats (n)	Peak flux Value (W/m^2)	Average Flux value (W/m^2)
10	5706.99	2658.02
11	6230.37	2890.60
12	6753.76	3123.17
13	7277.15	3355.75
14	7800.54	3588.33
15	8323.92	3820.91

As there is a variation of the flux on the receiver plate which will create the thermal stress and fatigue-creep failure. To avoid this, the allowable peak flux has to be carefully selected. Generally, one half to one-third of the peak flux is to be selected as an average flux [31]. The average flux is normally considered for sizing of the receiver so as to prevent its failure.

Based on the average value of the flux for each case a contour is plotted which is shown in Fig. 5. These contours show the area on the receiver plate in which average flux is falling. Based on this average flux contour, one can decide the size of the receiver.

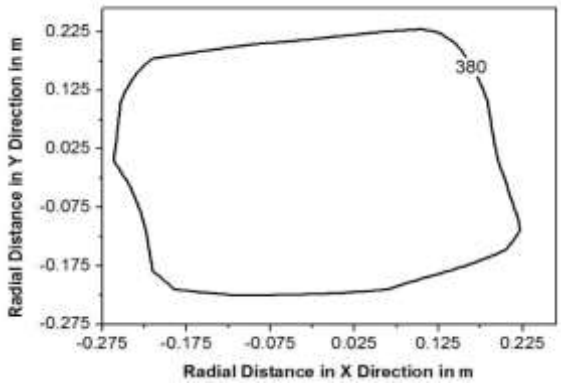

(a)

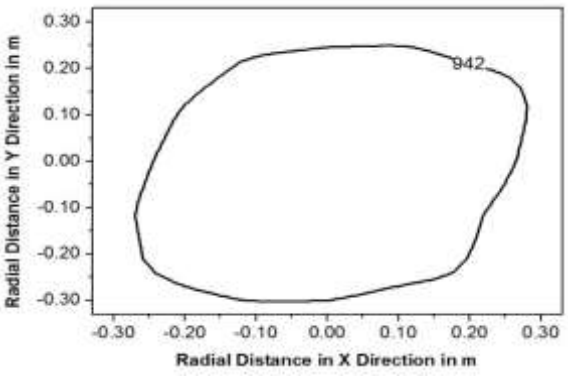

(b)

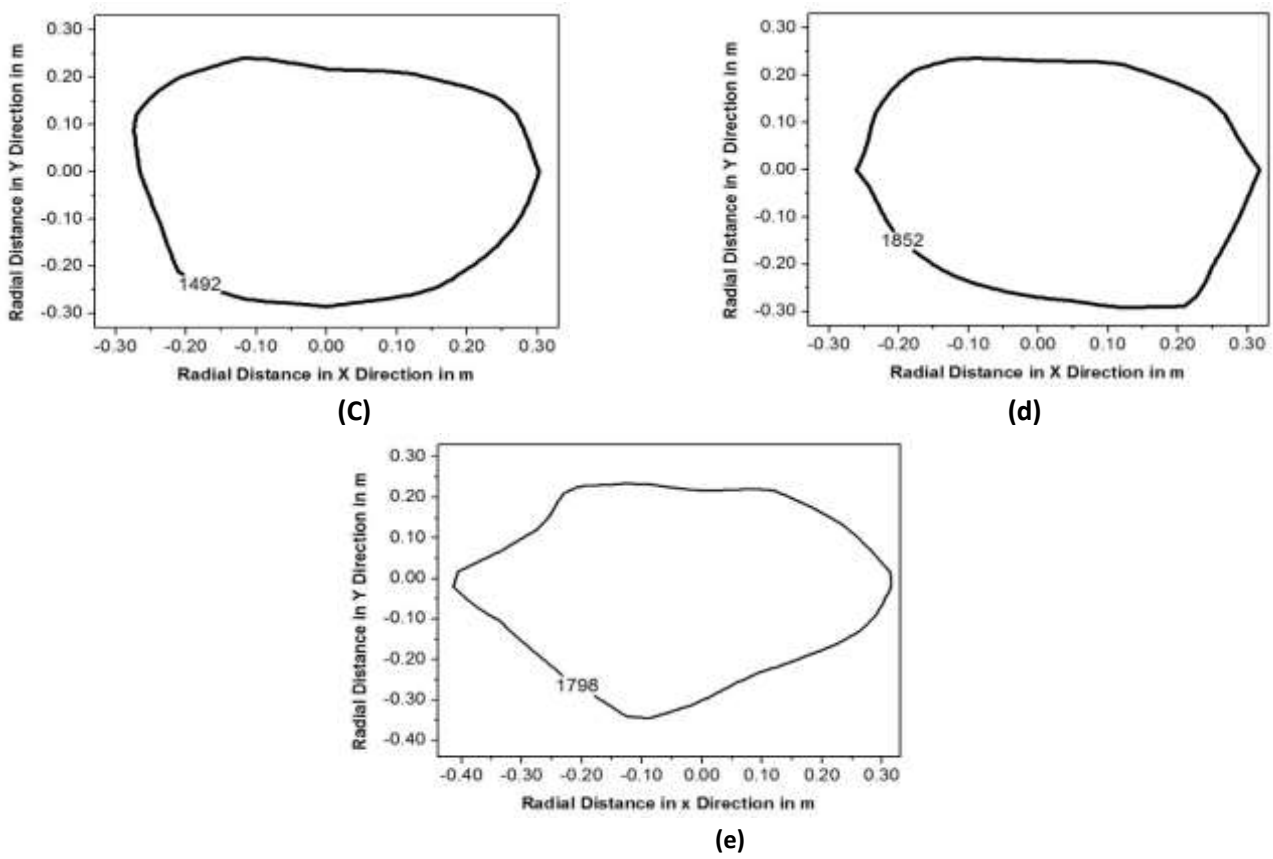

Fig. 5. Average Flux (W/m^2) contours on the receiver focusing **a.** One Heliostats **b.** Three heliostats **c.** Five Heliostats **d.** Seven Heliostats **e.** Nine Heliostats

For each case, the intercept factor was calculated. The intercept factor is the fraction of the flux falling on the receiver reflected from the heliostat system. In Table 3 the radius of the average contour, contour area and the intercept factor for each case is given. If the system is to be operated for the average flux value then the radius of the average flux can be taken as the receiver size.

From the Table 3, it is observed that the receiver size for the nine heliostat system with intercept factor 0.64 for the average flux value is 0.3 m x 0.3m.

Table 3. Receiver size based on average flux

Total Heliostats numbers focused	average flux (W/m^2)	The radius of the average flux contour (m)	Contour area for average flux (m^2)	Intercept factor
1	380	0.2	0.1794	0.59
3	942	0.3	0.2404	0.79
5	1492	0.3	0.2643	0.60
7	1852	0.3	0.2607	0.59
9	1798	0.3	0.2821	0.64

4.1. Analysis of the model heliostat system consisting of nine heliostats

For the model heliostat system by focusing all the nine heliostats the temperature profile on the focus plate varied from 180 to 215^{0}C at the center of the plate to about 120 to 140^{0}C at 0.3 m radius from the plate center. Optical concentration ratio was varying between 2.5 to 5.6. The maximum optical efficiency of the system was measured to be 0.50 ± 3 % during the test period. Fig. 6 shows the variation of the flux on the receiver plate in radial x and radial y-direction when all the nine heliostats were focused. From this Figs. 6 (a,b), it is seen that the maximum flux is obtained near the center of the plate and the flux density gradually decreases away from the center.

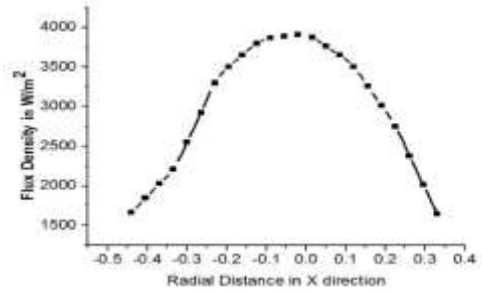

(a)

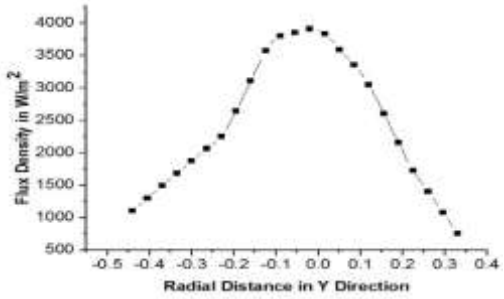

(b)

Fig. 6. Variation of the solar flux density (a) along the radial x and (b) along the radial y-direction

5. Conclusions

To evaluate the flux density distribution on the flat plate receiver of a model heliostat field a thermocouple method was used. This method is an indirect method of flux measurement. The variation of the solar flux density distribution on the receiver plate was estimated by using the energy balance equation for the different numbers of the heliostat. For each case, the time of the day was taken as the solar noon of that day.

For all the numbers of heliostats focused on the receiver plate, the peak solar flux value was obtained near the center of the receiver plate. The solar flux density is maximum near the center and it decreases gradually away from the center, which will cause the thermal stresses on the receiver plate. For such situations, a receiver which can sustain such a variation of the temperature has to be designed. For the nine heliostat system, the peak flux and average flux values are 3950.57 (± 3%) W/m^2 and 1798.77 (± 3%) W/m^2 respectively. The peak flux and the average flux value for fifteen heliostats in the first row predicted from the correlations are 8323.92 W/m^2 and 3820.91 W/m^2 respectively. For the average flux value on the receiver plate, the receiver size for the nine heliostats system will be 0.3m x 0.3m with the intercept factor of 64%. Optical concentration ratio was varying between 2.5 to 5.6. The optical efficiency of the system was measured to be 0.50 ± 3 % during the test period. By this analysis one can decide the size of the receiver based on average solar flux value.

Acknowledgments

The authors gratefully acknowledge the contribution and the facility provided by the Maharashtra Institute of Technology, Kothrud, Pune, India and Dr. Ravindra Patwardhan and M. D. Akole, from Akson Solar Equipment Private ltd., Bhor, Pune, India.

Nomenclature	
$\Phi_c(x)$	Solar flux at a distance 'x' from the center of the focus, [W/m^2]
h	Convective heat transfer coefficient of the focus plate, [W/m^2 K]
T_x	Temperature of the area element at radius 'x' from the center of the focus, [K]
T_{amb}	Ambient temperature, [K]
T_{sky}	Sky Temperature= $(T_{amb} - 6)$, [K]
k_i	Thermal conductivity of the insulation, [W/m-K]
t	Thickness of the insulation layer, [m]
σ	Stefan-Boltzmann constant, [W/m^{2}K^4]
ϵ	Emissivity of the plate
α	Absorptivity of the plate for solar radiation
$C(r_i)$	Local Concentration Ratio at radius (r_i) (m)
A_i	Area of the $'i^{th}'$ strip (m^2)
I_b	Normal beam radiation (W/m^2)
A	Aperture area of the concentrator (m^2)
n	Number of heliostats

References

[1] William B. Stine and Michael Geyer (2001): Power from the Sun. Available at, http://www.powerfromthesun.net/book.htm (2001), Ch. 10.

[2] J Ballestrín, G Burgess and J Cumpston. Heat flux and high-temperature measurement technologies for concentrating solar power (CSP). In: Concentrating solar power technology - developments and applications. Ed. K Lovegrove and W Stein. (Woodhead Publishing, 2012, 3-15)

[3] D. L. King, D. E. Arvizu, Heliostat Characterization at the Central Receiver Test facility, Transaction of ASME, 82, Vol. 103, May 1981.

[4] Strachan, J.W. and R.M. Houser, "Testing and Evaluation of Large-Area Heliostats for Solar Thermal Applications", SAND92-1381, Sandia National Laboratories, Albuquerque, NM,1993.

[5] Ulmer, S., W. Reinalter, P. Heller, E. Lupfert, and D. Martinez, "Beam Characterization and Improvement with a Flux Mapping System for Dish Concentrators", J. Solar Energy Engr., 124, pp. 182-188, 2002

[6] Zhe Dong, Xin Li, Wenfeng Liang, "Concentrated radiation measurement system for solar furnace", Power and Energy Engineering Conference (APPEEC), 2011 Asia-Pacific.

[7] O.A. Jaramillo, C.A. Perez-Rabago, C.A. Arancibia-Bulnes, C.A. Estrada, "A flat-plate calorimeter for concentrated solar flux evaluation", Renewable Energy 33 (2008) 2322–2328.

[8] Clifford K. Ho and Siri S. Khalsa, 2011, "A Flux Mapping Method For Central Receiver Systems", Proceedings of the ASME 2011 5th International Conference on Energy, Sustainability, Washington, DC, USA, pp. 743-751 August 7-10, 2011.

[9] A. Ibrahim, A. A. El-Sebaii, M. R. I. Ramadan, S. M. El-Broullesy, "Estimation of solar irradiance on inclined surfaces facing south in tanta, Egypt", International Journal of Renewable Energy Research, Vol. 1, No. 1, PP. 18-25, 2011

[10] Mehmet Demirtas, Mehmet Yesilbudak, Seref Sagiroglu and Ilhami Colak, "Prediction of solar radiation using meteorological data", International conference on Renewable Energy Research and Applications, ICRERA, Nagasaki, Japan, pp. 1-4, 11-14 Nov. 2012.

[11] Moein Jazayeri, Sener Uysal, Member, Kian Jazayeri, " A case study on solar data collection and effects of Sun's position in the sky on solar panel output characterization in Northern Cyprus", International conference on Renewable Energy Research and Applications, ICRERA, Madrid, Spain, pp. 184-189, 20-23 Oct. 2013.

[12] Xin-LinXia, Gui-LongDai, Yong Shuai, "Experimental and Numerical investigation on solar concentrating characteristics of sixteen-dish concentrator, International Journal of Hydrogen Energy", Volume 37, Issue 24, pp 18694-18703, December -2012.

[13] Kretzschmar, H., Gauché, P., Mouzouris, M., "Development of a Flat-Plate Calorimeter for a Small-scale Heliostat Field", SolarPaces, Marrakech, Morocco. 11- 14 September-2012

[14] Sebastian James Bode, Paul gauche, Willem Landman, 2012, "The design and testing of a small scale solar flux measurement system for central receiver plant", annual-student-symposium-2012, 23 November 2012.

[15] Emmanuel Guillot, Ivo Alxneit, Jesus Ballestrin, Jean Louis Sans, Christian Willsh, "Comparison of 3 heat flux gauges and a water calorimeter for concentrated solar irradiance measurement", Energy Procedia 49 pp. 2090 – 2099, 2014.

[16] Marc Roger, Patrik Herrmann, Steffen Ulmer, Miriam Ebert, Christoph Prahl, Felix Gohring, "Techniques to Measure Solar Flux Density Distribution on Large-Scale Receivers", Journal of Solar Energy Engineering, Vol. 136 / 031013-1-10 , August 2014.

[17] Hyunjin lee, Kwankyo Chai, Jongkyu Kim, sangnam Lee, hwanki Yoon, Chagkyun Yu, Yongheak kang, "Optical Performance Evaluation of a Solar Furnace by Measuring the highly Concentrated solar Flux", Energy, 66 , 63-69,2014.

[18] T. Kodamaa, N. Gokona, K. Matsubaraa, K. Yoshidaa, b, S. Koikarib,Y. Nagasec and K. Nakamurad, "Flux Measurement of a New Beam-down Solar Concentrating System in Miyazaki for Demonstration of Thermochemical Water Splitting Reactors", Energy Procedia 49 pp. 1990 – 1998, 2014.

[19] Miriam Ebert , Daniel Benitez , Marc Röger , Roman Korzynietz , José Antonio Brioso, "Efficiency determination of tubular solar receivers in central receiver systems", Solar Energy 139 pp. 179–189, 2016

[20] Rami Al-Hajj, Ali Assi, Farhan Batch, " An Evolutionary Computing Approach for estimating Global Solar Radiation", 5th International conference on Renewable Energy Research and Applications, ICRERA, Birmingham, UK, pp. 285-290, 20-23 Nov. 2016.

[21] Alain Ferriere, Mikael Volut, Antoine Perez and Yann Volut, "In-situ Measurement of Concentrated Solar Flux and Distribution at the Aperture of a Central Solar Receiver", SolarPACES 2015, AIP Conf. Proc. 1734, 130007-1–130007-8, 2015.

[22] Anita A. Nene, S. Ramchandran, "Numerical and Experimental Investigation of Scheffler concentrator Receiver for steam generation rate under different operating conditions", International Journal of Renewable Energy Research, Vol. 7, No. 4, PP. 2049-2056, 2017.

[23] Dhanesh Jain, Mahendra Lalwani, "A review on optimal inclination angles for solar arrays", International Journal of Renewable Energy Research, Vol. 7, No. 3, pp. 1053-1061,2017.

[24] Mohamed H. Ahmed, Mohamed Rady, Amr M A Amin, Fabio Maria Montagnino, Filippo Pardes, "Comparison of thermal and optical performance of linear Fresnel and parabolic trough concentrator", International Conference on Renewable Energy Research and Applications, ICRERA, Palermo, Italy, pp 626-629, 22-25 Nov. 2015.

[25] V. Rakeshsharma, S.J.Bhosale, S.B. Kedare, J.K.Nayak, 2005, "A simple method to determine optical quality of paraboloid concentrating solar thermal collector", Solar Energy Society of India (SESI) Journal, 15(2), pp.21-27, December 2005.

[26] C. A. Kinjavdekar, V. P. Muley, S. B Kedare and J. K. Nayak, 2010, "A Test Procedure for Determining Optical characteristics of a Dish Concentrator and its Implementation on Scheffler Dish", SESI Journal, 20(1) , pp. 13-23, December 2010.

[27] Ravindra Patwardhan, Rajiv Pandit, "Method and apparatus for orienting arrays of mechanically linked heliostats for focusing the incident sunlight on a stationary object", United States Patent Application, US 13/999,275 September 2014.

[28] Adan Al-Ghasem, Ghassan Tashtoush, MohammedAladeemy, "Experimental study of tracking 2-D compound parabolic concentrator(CPC) with flat plate absorber" International Conference on Renewable Energy Research and Applications, ICRERA, Madrid, Spain, pp 779-782, 20-23 Oct 2013.

[29] Wahiba Yaici,Evgueniy Entchev "Prediction of the performance of a solar energy system using neuro- Fuzzy interface system", International Conference on Renewable Energy Research and Applications, ICRERA, Milwaukee, WI,USA pp. 601-604, 19-22 Oct 2014.

[30] Evren M Toygar,Alpar Yazar, Tufan Byram,Mustafa Tustan, Omar Faruk Kaya, Ouzhan Das Huseyin Calmaz "Design and development of solar flat mirror and heat storage System" , International Conference on Renewable Energy Research and Applications, ICRERA, Milwaukee, WI, USA pp. 821-827, 19-22 Oct 2014.

[31] William B Stine and Raymond W Harrigan. "Solar energy fundamentals and design". Wiley Interscience 1985.